Palestine Journal of Mathematics

Vol. 12(4)(2023) , 410–424

ANALYSIS OF MICROPOLAR FLUID WITH NANOPARTICLES FLOW THROUGH A CORE REGION IN A STENOSED ARTERY HAVING MILD STENOSES

K. Maruthi Prasad, Bheema Sreekala and Prabhaker Reddy Yasa

Communicated by Suheel Khoury

MSC 2010 Classifications: Primary 92C10; Secondary 76Z05.

Keywords and phrases: Micropolar fluid, Stenosis, Peripheral Layer, Wall shear stress, Velocity of the fluid.

Abstract A theoretical model for the two layered micropolar fluid with nanoparticles flow through a stenosed artery is investigated. A two layered model is considered to represent the fluid flow passing through two regions (namely, Peripheral and Core) in a stenosed artery. The micropolar fluid with nanoparticles in core region acts as a non-Newtonian fluid and the fluid in peripheral layer is Newtonian fluid. The closed expressions of flow characteristics, like axial velocity profile, flow resistance, shear stress, temperature profile and concentration distribution are found to solve the governing equations using Homotopy Perturbation Method (HPM) with the assumption of mild stenosis. The impact of flow characteristics on the conformation to the flow, wall shear stress and velocity profiles are discussed graphically. A novel result is found that the resistance of fluid flow, shear at the wall and the axial velocity profile diminishes with the enhance of viscosity of fluid in the peripheral layer. Characteristics of temperature and concentration distribution due to the presence of micropolar fluid having nanoparticles in the core region has been studied to control the heat enhancement phenomenon. Streamlines are drawn to explore the fluid flow pattern and characteristics of momentum transfer.

1 Introduction

Experimental and theoretical analysis on fluid flows in small channels suggests that blood in certain flow conditions like low shear rates, acts as non-Newtonian fluid. It is known that the blood contains different types of cells, so that the viscous property of blood is changed and it shows non-Newtonian characteristics at shear rates in narrow elastic tube. The flow characteristics depends on the shape of the stenosis in artery, which is investigated by [1, 2]. Also, many investigations are available in the literature on the characteristics of blood flow, which explored the effect of structure in the arterial lumen of a blood channel [3, 4, 5, 6]. The effect of non-Newtonian fluid flowing across a non-uniform tube having multiple stenosis is studied by [7].

Erigen [8] introduced the theory of micropolar fluids, which is an effective model for the study of blood flow. These fluids contain hard, uniformly shaped (spherical) particles, suspended in a viscous layer that ignores particle deformation. Also, these types of fluids can help body couples and couple stresses while exhibiting micro rotational and inertial effects. The fluid substances rotation is taken care by a separate vector called the micro-rotation vector in micropolar fluid model. As a consequence, the micropolar fluid model might be more suitable for any bio-fluids. [9, 10, 11, 12, 13].

In many studies, it has been observed that the existence of a peripheral layer has been found to play a significant effect in functioning of arterial system [14]. The study of two-phase model for fluid flowing into stenotic channels in the existence of peripheral layer is done by [15]. The impact of the peripheral layer viscosity on the flow of blood into the arteries having mild stenosis is analysed by [16]. The blood flow of couple stress fluid in the stenotic arteries having peripheral layer is studied by [17].

With the foregoing points in view, a two-layered mathematical model for the fluid flow across a stenosed artery is considered. The effects of different fluid flow parameters on flow characteristics are analyzed by deriving the closed expression for resistance (or) flow Impedance and shear stress at wall by using Homotopy Perturbation Method under the purview of the assumptions of mild stenosis.

2 Mathematical Formulation

Consider the axisymmetric blood flow in a uniform circular cylinder with mild stenosis. The geometry of the stenosis is shown in Figure 1.

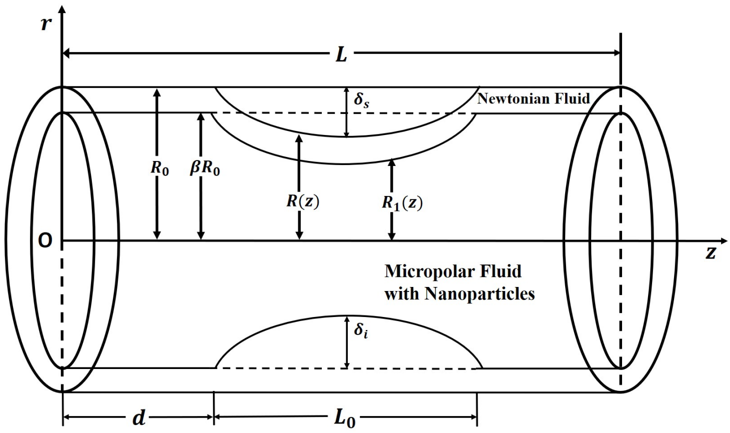

Figure 1. Geometry of arterial stenoses with peripheral layer

Radius of stenoses in the peripheral and core regions are [17]

$$h(z) = \frac{R(z)}{R_0} = \begin{cases} 1 - \frac{\delta_s}{2R_0}\left[1 + \cos\frac{2\pi}{L_0}\left(z - d - \frac{L_0}{2}\right)\right] & ; d \le z \le d + L_0 \\ 1 & ; \text{Otherwise} \end{cases} \tag{2.1}$$

$$h_1(z) = \frac{R_1(z)}{R_0} = \begin{cases} \beta - \frac{\delta_s}{2R_0}\left[1 + \cos\frac{2\pi}{L_0}\left(z - d - \frac{L_0}{2}\right)\right] & ; d \le z \le d + L_0 \\ \beta & ; \text{Otherwise} \end{cases} \tag{2.2}$$

Here $R(z)$ and $R_1(z)$ are respectively the radii of stenosed artery in peripheral and core regions. β is the proportion of the central radius to normal artery radius. Also, R_0 and βR_0 are radii of normal artery and core region of normal artery respectively. L_0, d are length and location of the stenoses. δ_s is the maximum altitude of the stenoses at $z = d + \frac{L_0}{2}$ such that $\frac{\delta_s}{R_0} << 1$ and $\frac{\delta_i}{R_0} << 1$.

The equations of motions in the peripheral region and core region are

a) **Peripheral Region**$(R_1(z) \le r \le R(z))$

$$\frac{\partial \bar{p}}{\partial \bar{z}} = \mu_p \nabla^2 \bar{w}_1 \tag{2.3}$$

$$\frac{\partial \bar{p}}{\partial \bar{r}} = 0 \tag{2.4}$$

where, $\nabla^2 \equiv \frac{\partial^2}{\partial r^2} + \frac{1}{r}\frac{\partial}{\partial r} + \frac{\partial^2}{\partial z^2}$, $\bar{w}_1$ is the component of velocity in the $\bar{z}$ direction, $\bar{p}, \mu_p$ are the pressure and constant velocity of Newtonian fluid in peripheral region.

b) **Core Region** $(0 \le r \le R_1(z))$

$$(\nabla \cdot W) = 0 \tag{2.5}$$

$$\rho(W \cdot \nabla W) = -(\nabla P) + (K\nabla \times W) + (\mu + K)\nabla^2 W \tag{2.6}$$

$$\rho j(W \cdot \nabla W) = -(2KV) + (K\nabla \times W) - \gamma(\nabla \times \nabla \times V) + (\alpha + \beta + \gamma)\nabla(\nabla \cdot V) \tag{2.7}$$

$$(\rho c)_f \frac{d\bar{T}}{dt} = k\nabla^2 \bar{T} + (\rho c)_p \left[D_{\bar{B}} \nabla \bar{C}.\nabla \bar{T} + \frac{D_{\bar{T}}}{\bar{T}_o} \nabla \bar{T}.\nabla \bar{T} \right] \tag{2.8}$$

$$\frac{d\bar{C}}{dt} = D_{\bar{B}} \nabla^2 \bar{C} + \left[\frac{D_{\bar{T}}}{\bar{T}_0} \right] \nabla^2 \bar{T} \tag{2.9}$$

Here, p, W, V, ρ, j are fluid pressure, Velocity vector, micro rotation vector, fluid density, micro gyration parameter respectively. $(\rho c)_f$, $(\rho c)_p$ are the density of the fluid and density of the fluid and density of the particle respectively. $\frac{d}{dt}$ represents the material time derivative, $\bar{C}$ is nanoparticle phenomena, $D_{\bar{T}}$ and $D_{\bar{B}}$ are the thermophoretic and Brownian diffusion coefficients respectively. Also, as $\bar{r}$ tends to $\bar{h}$, the values of $\bar{T}$ and $\bar{C}$ are $\bar{T}_0$ and $\bar{C}_0$. k, α, β, γ are material constants and satisfies the following inequalities [8]

$$2\mu + K \geq 0, 3\alpha + \beta \geq 0, \gamma \geq |\beta|$$

Since, the flow is axisymmetric, every variable is independent of θ. Therefore, W=$(w_r, 0, w_z)$ and V=$(0, v_\theta, 0)$ are velocity and microrotation vectors respectively.

Introducing the following non-dimensional variables
$r = \frac{\bar{r}}{R_0}$, $z = \frac{\bar{z}}{\lambda}$, $w_r = \frac{\lambda \bar{w}_r}{cR_0}$, $w_z = \frac{\bar{w}_z}{c}$, $p = \frac{R_0^2 \bar{p}}{c\lambda\mu_c}$, $\theta_t = \frac{\bar{T} - \bar{T}_0}{\bar{T}_0}$, $t = \frac{c\bar{t}}{\lambda}$, $\sigma = \frac{\bar{C} - \bar{C}_0}{\bar{C}_0}$, $\alpha = \frac{k}{(\rho c)_f}$, $N_b = \frac{(\rho c)_p D_{\bar{B}} \bar{C}_0}{(\rho c)_f}$, $N_t = \frac{(\rho c)_p D_{\bar{T}} \bar{T}_0}{(\rho c)_f \alpha}$, $G_r = \frac{g\alpha \bar{T}_0 R_0^3}{\varphi^2}$, $B_r = \frac{g\alpha \bar{C}_0 R_0^3}{\varphi^2}$, $\varphi^2 = \frac{\mu_c}{\rho}$, $\delta = \frac{R_0}{\lambda}$

Where, θ_t, σ, N_t, N_b, B_r and G_r are respectively temperature profile, nano particle phenomenon, Thermophoresis parameter, Brownian motion parameter, local nanoparticle Grashof number and local temperature Grashof number.

The governing equations are

$$\frac{\partial p}{\partial z} = \frac{1}{r} \frac{\partial}{\partial r} \left(\bar{\mu} r \frac{\partial}{\partial r} \right) w_1 \tag{2.10}$$

$$\frac{\partial p}{\partial r} = 0 \tag{2.11}$$

$$\frac{N}{r} \frac{\partial}{\partial r}(rv_\theta) + \frac{\partial^2 w}{\partial r^2} + \frac{1}{r} \frac{\partial w}{\partial r} + (1 - N)\frac{\sin \alpha}{F} + (1 - N)(G_r \theta_t + B_r \sigma) = (1 - N)\frac{\partial P}{\partial z} \tag{2.12}$$

$$2v_\theta + \frac{\partial w}{\partial r} - \frac{2 - N}{m^2} \frac{\partial}{\partial r} \left(\frac{1}{r} \frac{\partial}{\partial r}(rv_\theta) \right) = 0 \tag{2.13}$$

$$\frac{1}{r} \frac{\partial}{\partial r} \left(r \frac{\partial \theta_t}{\partial r} \right) + N_b \frac{\partial \sigma}{\partial r} \frac{\partial \theta_t}{\partial r} + N_t \left(\frac{\partial \theta_t}{\partial r} \right)^2 = 0 \tag{2.14}$$

$$\frac{1}{r} \frac{\partial}{\partial r} \left(r \frac{\partial \sigma}{\partial r} \right) + \frac{N_t}{N_b} \left(\frac{1}{r} \frac{\partial}{\partial r} \left(r \frac{\partial \theta_t}{\partial r} \right) \right) = 0 \tag{2.15}$$

Where, w_z is the velocity along the axial direction. Here, $m^2 = \frac{{R_0}^2 k(2\mu_c + k)}{\gamma(\mu_c + k)}$ is micropolar parameter and $N = \frac{k}{\mu_c + k}$ is the coupling number $(0 \leq N < 1)$.

The non-dimensional boundary conditions are

$$w_1 = -1 \text{ at } r = h(z) \tag{2.16}$$

$$\frac{\partial w_z}{\partial r} = 0\,,\ \frac{\partial \theta_t}{\partial r} = 0,\ \frac{\partial \sigma}{\partial r} = 0 \text{ at } r = 0 \tag{2.17}$$

$$v_\theta = 0,\ \theta_t = 0\,,\ \sigma = 0 \text{ at } r = h_1(z) \tag{2.18}$$

$$v_\theta \text{ is finite}, w_z \text{ is finite at } r = h_1(z) \tag{2.19}$$

$$w_1 = w_z, \text{ at } r = h_1(z) \tag{2.20}$$

$$\bar{\mu}\,\frac{\partial w_1}{\partial r} = \frac{\partial w_z}{\partial r} - \frac{N}{1-N} v_\theta + \frac{r}{2}\left(G_r\theta_t + B_r\sigma\right) \text{ at } r = h_1(z) \tag{2.21}$$

3 Solution of the Problem

The expression for w_1 from the equation (2.10) and (2.16) is

$$w_1 = \frac{r^2 - h^2}{4\bar{\mu}}\frac{dp}{dz} + \frac{c_1}{\bar{\mu}}\log\left(\frac{r}{h}\right) \tag{3.1}$$

By applying HPM, the solutions of Equations (2.14) and (2.15) are

$$H\left(q_t, \theta_t\right) = \left(1 - q_t\right)\left[L\left(\theta_t\right) - L\left(\theta_{10}\right)\right] + q_t\left[L\left(\theta_t\right) + N_b\frac{\partial\sigma}{\partial r}\frac{\partial\theta_t}{\partial r} + N_t\left(\frac{\partial\theta_t}{\partial r}\right)^2\right] \tag{3.2}$$

$$H\left(q_t, \sigma\right) = \left(1 - q_t\right)\left[L\left(\sigma\right) - L\left(\sigma_{10}\right)\right] + q_t\left[L\left(\sigma\right) + \frac{N_t}{N_b}\left(\frac{1}{r}\frac{\partial}{\partial r}\left(r\frac{\partial\theta_t}{\partial r}\right)\right)\right] \tag{3.3}$$

Where, q_t is the embedding parameter $(0 \le q_t \le 1)$. $L \equiv \frac{1}{r}\frac{\partial}{\partial r}\left(r\frac{\partial}{\partial r}\right)$ is a linear operator. θ_{10} and σ_{10} are the initial guesses, given as

$$\theta_{10}\left(r, z\right) = \left(\frac{r^2 - h^2}{4}\right),\quad \sigma_{10}\left(r, z\right) = -\left(\frac{r^2 - h^2}{4}\right) \tag{3.4}$$

$$\theta_t\left(r, z\right) = \theta_{t_0} + q_t\theta_{t_1} + q_t^2\theta_{t_2} + \ \ldots \tag{3.5}$$

$$\sigma\left(r, z\right) = \sigma_0 + q_t\sigma_1 + q_t^2\sigma_2 + \ \ldots \tag{3.6}$$

Convergence of equations (3.5) and (3.6) depend on the non-linear part of the expression. For $q_t = 1$, the solution for temperature and nanoparticle phenomena is

$$H\left(q, \theta\right) = L\left(\theta\right) - L\left(\theta_{10}\right) + qL\left(\theta_{10}\right) + q\left[N_b\left(\frac{\partial\sigma}{\partial r}\frac{\partial\theta_t}{\partial r}\right) + N_t\left(\frac{\partial\theta_t}{\partial r}\right)^2\right] \tag{3.7}$$

$$H\left(q, \sigma\right) = L\left(\sigma\right) - L\left(\sigma_{10}\right) + qL\left(\sigma_{10}\right) + q\left[\frac{N_t}{N_b}\frac{1}{r}\frac{\partial}{\partial r}\left(r\frac{\partial\theta_t}{\partial r}\right)\right] \tag{3.8}$$

The solution for temperature profile and nano particle phenomena for $q = 1$ is

$$\theta_t\left(r, z\right) = \frac{\left(N_b - N_t\right)}{64}\left(r^2 - h^2\right) - \frac{N_b}{18}\left(r^3 - h^3\right) - \frac{N_t\left({N_b}^2 + {N_t}^2\right)}{36864}\left(r^4 - h^4\right)\left(r^6 - h^6\right) \tag{3.9}$$

$$\sigma(r,z) = -\frac{\left(r^2-h^2\right)}{4}\frac{N_t}{N_b} + \frac{N_t}{N_b}\left(\frac{N_b}{18}\left(r^3-h^3\right) + \frac{\left({N_b}^2+{N_t}^2\right)}{36864}\left(r^6-h^6\right)\right) \tag{3.10}$$

Substituting equations (3.9) and (3.10) in (2.13) and applying boundary conditions

$$\frac{\partial}{\partial r}\left[Nrv_\theta + r\frac{\partial w_z}{\partial r} + \frac{N-1}{2}r^2\frac{dP}{dz}\right] = (1-N)\left[G_r\left(\frac{1}{64}(N_b-N_t)\left(r^3-r{h_1}^2\right) - \left(\frac{N_b}{18}\left(r^4-r{h_1}^3\right) + \frac{N_t\left({N_b}^2+{N_t}^2\right)}{36864}\left(r^5-r{h_1}^4\right)\left(r^6-{h_1}^6\right)\right)\right) + B_r\left(-\frac{N_t}{N_b}\frac{\left(r^3-r{h_1}^2\right)}{4} + \frac{N_t}{N_b}\left(\frac{N_b}{18}\left(r^4-r{h_1}^3\right) + \frac{\left({N_b}^2+{N_t}^2\right)}{36864}\left(r^7-r{h_1}^6\right)\right)\right)\right] \tag{3.11}$$

From equations (3.9), (3.10) and (2.13) expression for v_θ can be written as

$$\frac{\partial^2 v_\theta}{\partial r^2} + \frac{1}{r}\frac{\partial v_\theta}{\partial r} - \left(m^2+\frac{1}{r^2}\right)v_\theta = \frac{1-N}{2-N}m^2\left[\frac{r}{2}\frac{dP}{dz} + \frac{G_r(N_b-N_t)}{64}\left(\frac{r^3}{4}-\frac{rh_1^2}{2}\right) - \frac{G_rN_b}{18}\left(\frac{r^4}{5}-\frac{rh_1^3}{2}\right) - \frac{G_rN_t\left({N_b}^2+{N_t}^2\right)}{36864}\left(\frac{r^{11}}{12}-\frac{r^5h_1^6}{6}-\frac{r^7h_1^4}{8}+\frac{rh_1^{10}}{2}\right) - \frac{B_r}{4}\frac{N_t}{N_b}\left(\frac{r^3}{4}-\frac{rh_1^2}{2}\right) + \frac{B_r}{18}N_t\left(\frac{r^4}{5}-\frac{rh_1^3}{2}\right) + B_r\frac{N_t}{N_b}\frac{{N_b}^2+{N_t}^2}{36864}\left(\frac{r^7}{8}-\frac{rh_1^6}{2}\right)\right] \tag{3.12}$$

The general solution of equation (3.11) is

$$v_\theta = c_4(z)\ I_1(mr) + c_5(z)\ K_1(mr) + \frac{N-1}{2-N}\left[\frac{r}{2}\frac{dP}{dz} + G_r(N_b-N_t)\left(\frac{r}{32m^2}-\frac{rh_1^2}{128}+\frac{r^3}{256}\right) - G_rN_b\left(\frac{1}{2m^4}-\frac{rh_1^3}{36}+\frac{r^2}{6m^2}+\frac{r^4}{90}\right) - \frac{G_rN_t\left({N_b}^2+{N_t}^2\right)}{36864}\left(\frac{7372800r}{m^{10}}-\frac{1152rh_1^4}{m^6}-\frac{32rh_1^6}{m^4}+\frac{rh_1^{10}}{2}+\frac{921600}{m^8}r^3-\frac{144}{m^4}r^3h_1^4-\frac{4r^3h_1^6}{m^2}+\frac{38400r^5}{m^6}-\frac{6r^5h_1^4}{m^2}-\frac{r^5h_1^6}{6}+\frac{800r^7}{m^4}-\frac{r^7h_1^4}{8}+\frac{10r^9}{m^2}+\frac{r^{11}}{12}\right) - B_r\frac{N_t}{N_b}\left(\frac{r}{2m^2}-\frac{rh_1^2}{8}+\frac{r^3}{16}\right) - B_rN_t\left(\frac{-1}{2m^4}+\frac{rh_1^3}{36}-\frac{r^2}{6m^2}-\frac{r^4}{90}\right) + B_r\frac{N_t}{N_b}\frac{\left({N_b}^2+{N_t}^2\right)}{36864}\left(\frac{1152r}{m^6}-\frac{rh_1^6}{2}+\frac{144r^3}{m^4}+\frac{6r^5}{m^2}+\frac{r^7}{8}\right)\right] \tag{3.13}$$

where, $I_1(mr)$ and $K_1(mr)$ are respectively the first and second order modified Bessel functions. From equations (3.12), (3.13) and by applying boundary conditions (2.17)-(2.21)

$$w_z = -Nc_4\frac{I_0(mr)}{m} + \frac{1-N}{2-N}\left[\frac{r^2}{2}\frac{dP}{dz} + G_r(N_b-N_t)\left(\frac{Nr^2}{64m^2}+\frac{r^4}{512}-\frac{r^2h_1^2}{128}\right) + G_rN_b\left(\frac{-Nr}{2m^4}-\frac{Nr^3}{18m^2}-\frac{r^5}{225}+\frac{r^2h_1^3}{36}\right) + \frac{G_rN_t\left({N_b}^2+{N_t}^2\right)}{36864}\left(\frac{-3686400Nr^2}{m^{10}}-\frac{230400Nr^4}{m^8}+\frac{576Nr^2h_1^4}{m^6}-\frac{6400Nr^6}{m^6}+\frac{16Nr^2h_1^6}{m^4}+\frac{36Nr^4h_1^4}{m^4}-\frac{100Nr^8}{m^4}+\frac{Nr^4h_1^6}{m^2}-\frac{Nr^{10}}{m^2}+\frac{Nr^6h_1^4}{m^2}-\frac{r^{12}}{72}+\frac{r^6h_1^6}{18}+\frac{r^8h_1^4}{32}-\frac{r^2h_1^{10}}{2}\right) + B_r\frac{N_t}{N_b}\left(\frac{-Nr^2}{4m^2}-\frac{r^4}{32}+\frac{r^2h_1^2}{8}\right) + B_rN_t\left(\frac{Nr}{2m^4}+\frac{Nr^3}{18m^2}+\frac{r^5}{225}-\frac{r^2h_1^3}{36}\right) + B_r\frac{N_t}{N_b}\frac{\left({N_b}^2+{N_t}^2\right)}{36864}\left(\frac{576Nr^2}{m^6}+\frac{36Nr^4}{m^4}+\frac{Nr^6}{m^2}+\frac{r^8}{32}-\frac{r^2h_1^6}{2}\right)\right] + c_6 \tag{3.14}$$

Where,

$$c_1 = -Nh_1^2\frac{dP}{dz} - \frac{N(2-N)}{1-N}h_1A + B$$

$$c_4 = \frac{1}{I_1(mh_1)}\left[\frac{1-N}{2-N}\,\frac{h_1}{2}\,\frac{dP}{dz} + A\right]$$

$$c_6 = \frac{dP}{dz}\left[\frac{N}{m}\,\frac{I_0(mh_1)}{I_1(mh_1)}\left(\frac{1-N}{2-N}\right)\frac{h_1}{2} - \frac{Nh_1^2}{2\bar{\mu}}\log\frac{h_1}{h} + \frac{h_1^2}{4\bar{\mu}} - \frac{h^2}{4\bar{\mu}} + \left(\frac{N-1}{2-N}\right)\frac{h_1^2}{2}\right] + \frac{N}{m}\frac{I_0(mh_1)}{I_1(mh_1)}A - \frac{N(2-N)}{1-N}\frac{h_1A}{\bar{\mu}}\log\frac{h_1}{h} + \frac{B}{\bar{\mu}}\log\frac{h_1}{h} + C - 1$$

$$A = \frac{1-N}{2-N}\Bigg[G_r(N_b-N_t)\left(\frac{h_1}{32m^2} - \frac{h_1^3}{256}\right) + G_rN_b\left(\frac{-1}{2m^4} - \frac{h_1^2}{6m^2} + \frac{h_1^4}{60}\right) + G_rN_t \frac{\left({N_b}^2+{N_t}^2\right)}{36864}\left(\frac{-7372800h_1}{m^{10}} - \frac{37248h_1^5}{m^6} - \frac{624h_1^7}{m^4} - \frac{7h_1^{11}}{24} - \frac{921600}{m^8}h_1^3\right) + B_r\frac{N_t}{N_b}\left(\frac{-h_1}{2m^2} + \frac{h_1^3}{16}\right) + B_rN_t\left(\frac{1}{2m^4} + \frac{h_1^2}{6m^2} - \frac{h_1^4}{60}\right) + B_r\frac{N_t}{N_b}\frac{\left({N_b}^2+{N_t}^2\right)}{36864} \left(\frac{1152h_1}{m^6} + \frac{144h_1^3}{m^4} - \frac{3h_1^7}{8} + \frac{6h_1^5}{m^2}\right)\Bigg]$$

$$B = \frac{1}{2-N}G_r(N_b-N_t)\left(\frac{Nh_1^2}{16m^2} + \frac{Nh_1^4}{256} - \frac{h_1^4}{128} - \frac{N^2h_1^2}{32m^2}\right) + \frac{G_rN_b}{2-N}\Bigg(-\frac{Nh_1}{m^4} - \frac{Nh_1^3}{3m^2} + \frac{N^2h_1}{2m^4} + \frac{N^2h_1^3}{6m^2} + \frac{h_1^5}{30} - \frac{Nh_1^5}{60}\Bigg) + \frac{G_rN_t\left({N_b}^2+{N_t}^2\right)}{(2-N)\,36864}\Bigg(-\frac{14745600Nh_1^2}{m^{10}} - Nh_1^4 \frac{1843200}{m^8} + \frac{37248N^2h_1^6}{m^6} + \frac{624Nh_1^8}{m^4} + \frac{7Nh_1^{12}}{24}\Bigg) + \frac{B_r}{2-N}\,\frac{N_t}{N_b}\Bigg(\frac{-Nh_1^2}{m^2} + \frac{N^2h_1^2}{2m^2} + \frac{h_1^4}{8} - \frac{Nh_1^4}{16}\Bigg) + \frac{B_rN_t}{2-N}\left(\frac{Nh_1}{m^4} + \frac{Nh_1^3}{3m^2} - \frac{N^2h_1^3}{6m^2} - \frac{37h_1^5}{60} - \frac{N^2h_1}{2m^4} + \frac{3Nh_1^5}{5}\right) + \frac{B_r}{2-N}\frac{N_t}{N_b}\frac{\left({N_b}^2+{N_t}^2\right)}{36864}\Bigg(\frac{2304Nh_1^2}{m^6} + \frac{288Nh_1^4}{m^4} + \frac{12Nh_1^6}{m^2} - \frac{3h_1^8}{4} - \frac{1152N^2h_1^2}{m^6} - \frac{144N^2h_1^4}{m^4} - \frac{6N^2h_1^6}{m^2} + \frac{3Nh_1^8}{8}\Bigg)$$

$$C = \frac{N-1}{2-N}\Bigg[G_r(N_b-N_t)\left(\frac{Nh_1^2}{64m^2} - \frac{3h_1^4}{512}\right) + G_rN_b\left(-\frac{Nh_1}{2m^4} - \frac{Nh_1^3}{18m^2} + \frac{7h_1^5}{300}\right) + \frac{G_rN_t\left({N_b}^2+{N_t}^2\right)}{36864}\Bigg(\frac{-3686400Nh_1^2}{m^{10}} - \frac{230400Nh_1^4}{m^8} - \frac{5824Nh_1^6}{m^6} - \frac{48Nh_1^8}{m^4} + \frac{Nh_1^{10}}{m^2} - \frac{41}{96}h_1^{12}\Bigg) + B_r\,\frac{N_t}{N_b}\left(\frac{-Nh_1^2}{m^2} + \frac{3h_1^4}{32}\right) + B_rN_t\left(\frac{Nh_1}{2m^4} + \frac{Nh_1^3}{18m^2} - \frac{7h_1^5}{300}\right) + B_r\frac{N_t}{N_b}\frac{\left({N_b}^2+{N_t}^2\right)}{36864}\left(\frac{576Nh_1^2}{m^6} + \frac{36Nh_1^4}{m^4} + \frac{Nh_1^6}{m^2} - \frac{15h_1^8}{32}\right)\Bigg]$$

The dimension less flux (q) is

$$q = \int_0^{h_1} 2rw\, dr + \int_{h_1}^{h} 2rw_1\, dr \tag{3.15}$$

Substituting w_1 and w_z from equations (3.1) and (3.14) in (3.15)

$$q = \frac{dp}{dz}\Bigg[-\frac{N}{m}\left(\frac{1-N}{2-N}\right)hh_1 - \left(\frac{1-N}{2-N}\right)\frac{h_1^4}{4} + \frac{N}{m}\frac{I_0(mh_1)}{I_1(mh_1)}\left(\frac{1-N}{2-N}\right)\frac{h_1^3}{2} + \frac{3h_1^4}{8\bar{\mu}} + \left(\frac{N-1}{2-N}\right)\frac{h_1^4}{8\bar{\mu}} - \frac{h^4}{8\bar{\mu}} - \frac{Nh_1^4}{4\bar{\mu}} + \frac{Nh^2h_1^2}{4\bar{\mu}}\Bigg] + A\Bigg[\frac{-2Nh}{m} + \frac{N}{m}\frac{I_0(mh_1)}{I_1(mh_1)}h_1^2 - N\left(\frac{2-N}{1-N}\right)\frac{h_1\left(h_1^2-h^2\right)}{2\bar{\mu}}\Bigg] + \frac{B\left(h_1^2-h^2\right)}{2\bar{\mu}} + Ch_1^2 + D - h^2 \tag{3.16}$$

where,

$$D = \frac{1-N}{2-N}\Bigg[G_r(N_b-N_t)\left(\frac{Nh_1^4}{128m^2} - \frac{5h_1^6}{1536}\right) + G_rN_b\left(-\frac{Nh_1^3}{3m^4} - \frac{Nh_1^5}{45m^2} + \frac{53h_1^7}{4200}\right) + G_r N_t\frac{\left(N_b{}^2+N_t{}^2\right)}{36864}\left(\frac{-1843200Nh_1^4}{m^{10}} - \frac{76800Nh_1^6}{m^8} - \frac{1312Nh_1^8}{m^6} + \frac{5Nh_1^{12}}{12m^2} - \frac{779}{3360}h_1^{14}\right) + B_r\frac{N_t}{N_b}\left(\frac{-Nh_1^4}{8m^2} + \frac{5h_1^6}{96}\right) + B_rN_t\left(\frac{Nh_1^3}{3m^4} + \frac{Nh_1^5}{45m^2} - \frac{53h_1^7}{4200}\right) + B_r\frac{N_t}{N_b}\frac{\left(N_b{}^2+N_t{}^2\right)}{36864}\left(\frac{288Nh_1^4}{m^6} + \frac{12Nh_1^6}{m^4} + \frac{Nh_1^8}{4m^2} - \frac{39h_1^{10}}{160}\right)\Bigg]$$

From equation (3.16), $\frac{dp}{dz}$ is

$$\frac{dp}{dz} = \frac{1}{S}\Bigg[q - A\left[\frac{-2Nh}{m} + \frac{N}{m}\frac{I_0(mh_1)}{I_1(mh_1)}h_1^2 - N\left(\frac{2-N}{1-N}\right)\frac{h_1\left(h_1^2-h^2\right)}{2\bar{\mu}}\right] - B\frac{\left(h_1^2-h^2\right)}{2\bar{\mu}} - Ch_1^2 - D + h^2\Bigg] \tag{3.17}$$

where,

$$S = -\frac{N}{m}\left(\frac{1-N}{2-N}\right)hh_1 + \left(\frac{N-1}{2-N}\right)\frac{h_1^4}{4} + \frac{N}{m}\frac{I_0(mh_1)}{I_1(mh_1)}\frac{h_1^3}{2} + \frac{3h_1^4}{8\bar{\mu}} + \left(\frac{N-1}{2-N}\right)\frac{h_1^4}{2} - \frac{h^4}{8\bar{\mu}} - \frac{Nh_1^4}{4\bar{\mu}} + \frac{Nh^2h_1^2}{4\bar{\mu}} \tag{3.18}$$

The pressure drop per wave length is ΔP_λ is

$$\Delta P_\lambda = -\int_0^1 \frac{dP}{dz}dz \tag{3.19}$$

On substituting $\frac{dP}{dz}$, the pressure drop is $\Delta P_\lambda = qL_1 + L_2$ where,

$$L_1 = -\int_0^1 \frac{1}{S}\,dz$$

$$L_2 = \int_0^1 \frac{1}{S}\Bigg[A\left[\frac{-2Nh}{m} + \frac{N}{m}\frac{I_0(mh_1)}{I_1(mh_1)}h_1^2 - N\left(\frac{2-N}{1-N}\right)\frac{h_1\left(h_1^2-h^2\right)}{2\bar{\mu}}\right] + B\frac{\left(h_1^2-h^2\right)}{2\bar{\mu}} + Ch_1^2 + D - h^2\Bigg]dz$$

The flow impedance is

$$\lambda = \frac{\Delta P_\lambda}{q} \tag{3.20}$$

The shearing stress acting at the wall is

$$\tau_R = -\frac{h}{2}\frac{dp}{dz} \tag{3.21}$$

Wall shear stress at the maximum altitude of the stenoses, i.e., $z = d + \frac{L_0}{2}$ is

$$\tau_s = \left(-\frac{h}{2}\frac{dp}{dz}\right)_{h=1-\frac{\delta_s}{R_0}} \tag{3.22}$$

Also, $R_1 = \beta R$ and $\delta_i = \beta\delta_s$.

The dimensionless flow impedance $\bar{\lambda}$ and shearing stress $\bar{\tau}_s$ acting at wall are

$$\bar{\lambda} = \frac{\lambda}{\lambda_c}, \bar{\tau}_s = \frac{\tau_s}{\tau_c} \tag{3.23}$$

where, λ_c and τ_c are respectively, the flow resistance and wall shear stress in the absence of the peripheral layer for the normal artery.

4 Results and Discussions

It is noted from Figures (2 - 11) that flow Impedance enhances with increase of heights of the stenoses, B_r, m and β, but decreases with increase of G_r, N_t, N_b, q and μ . Also, Influence of fluid flow parameters on wall shear stress $(\bar{\tau}_s)$ are shown in figures (12 - 20). It may be noted that shear stress at the wall found increases with increase of G_r, N_t, N_b, β and μ, but decreases with stenosis heights, B_r, m and q and are shown in figures.
The effects of velocity profiles in core region can be seen in Figures (21 - 28). It is noted that, the axial velocity profiles increase in the radial direction with the rise of β, q and stenoses height, but decreases with the increase of B_r, G_r, N_b, N_t and μ.
Figures (29 - 30), concentration is decreases with N_b, but increases with N_t. It is also noticed that Temperature profile increases by enhancing N_t, whereas it decreases by enhancing N_b and is illustrated in figures (31 - 32).
Figures (33 - 36) displays the streamlines for distinct values of β, μ, q and δ_s. It is seen that, with the rise of values of β, the area of the boluses expands, but the number of boluses are decreased. Also, it is observed that, the area of the boluses enlarges and the number of bolus are increased with increase of viscosity (μ) of the fluid and flux. It is also noted that, with the increase of stenosis height of core region, the area of bolus is decreased, but number of bolus is increased.

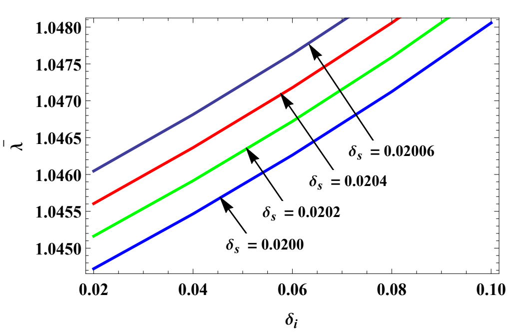

Figure 2. Variation of δ_i on $\bar{\lambda}$ as δ_s varies

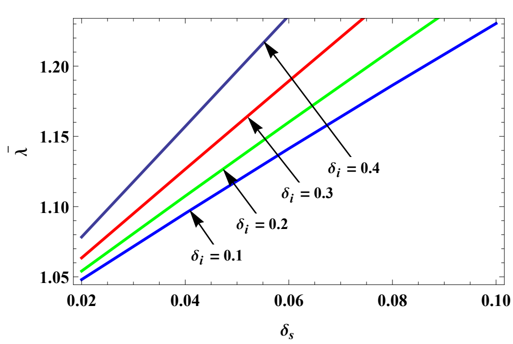

Figure 3. Variation of δ_s on $\bar{\lambda}$ as δ_i varies

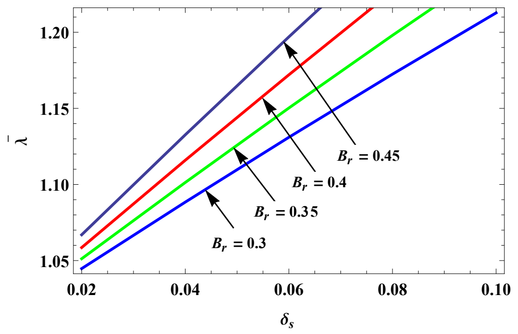

Figure 4. Variation of δ_s on $\bar{\lambda}$ as B_r varies

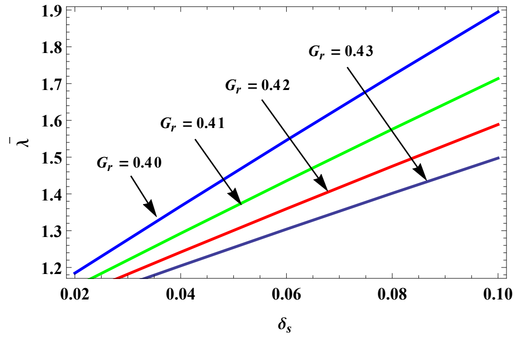

Figure 5. Variation of δ_s on $\bar{\lambda}$ as G_r varies

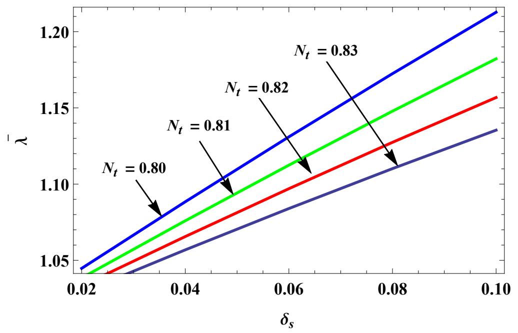

Figure 6. Variation of δ_s on $\bar{\lambda}$ as N_t varies

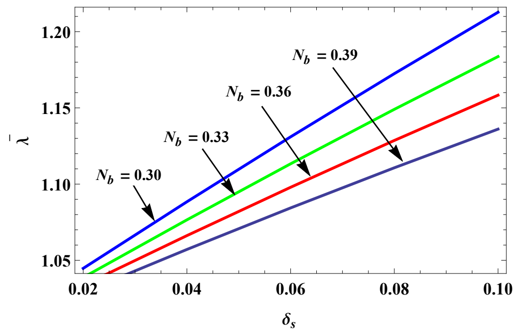

Figure 7. Variation of δ_s on $\bar{\lambda}$ as N_b varies

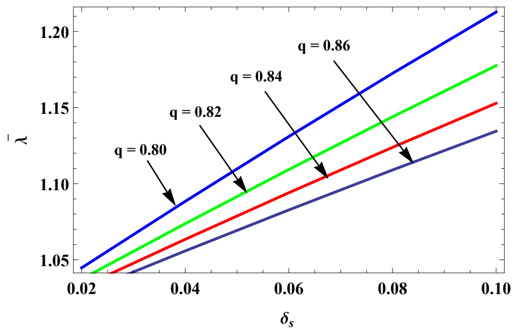

Figure 8. Variation of δ_s on $\bar{\lambda}$ as q varies

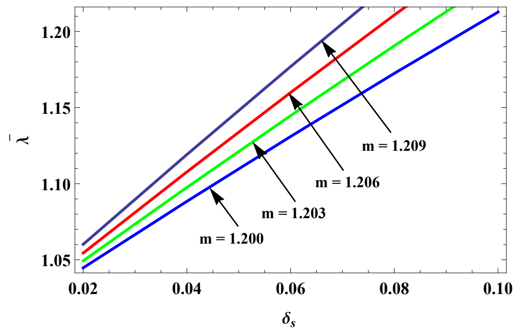

Figure 9. Variation of δ_s on $\bar{\lambda}$ as m varies

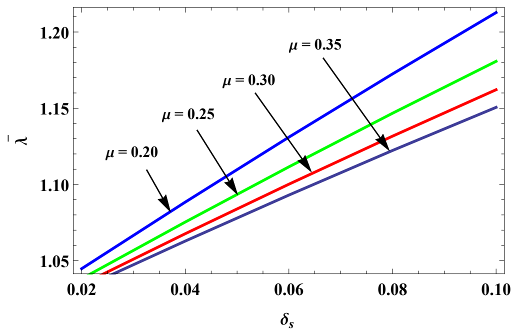

Figure 10. Effect of δ_s on $\bar{\lambda}$ as μ varies

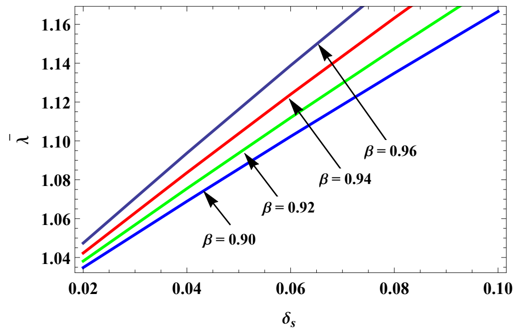

Figure 11. Effect of δ_s on $\bar{\lambda}$ as β varies

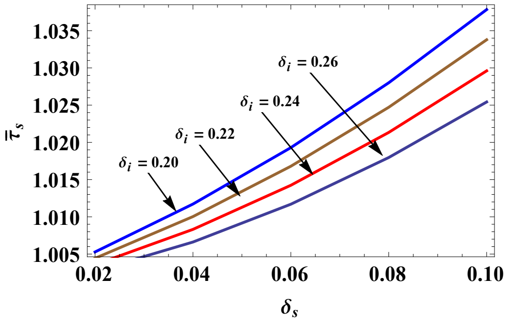

Figure 12. Effect of δ_s on $\bar{\tau}_s$ as δ_i varies

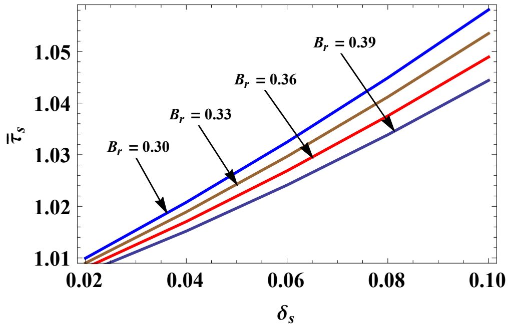

Figure 13. Effect of δ_s on $\bar{\tau}_s$ as B_r varies

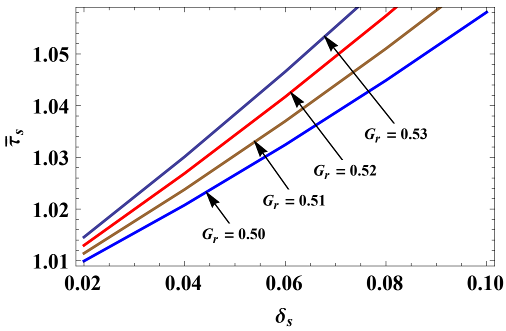

Figure 14. Effect of δ_s on $\bar{\tau}_s$ as G_r varies

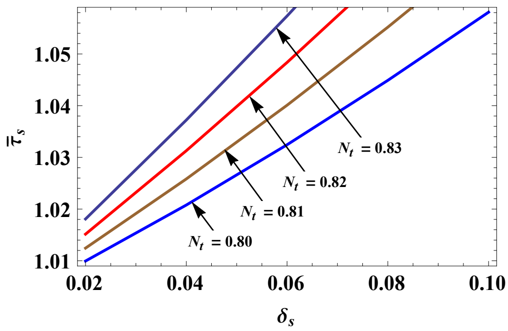

Figure 15. Effect of δ_s on $\bar{\tau}_s$ as N_t varies

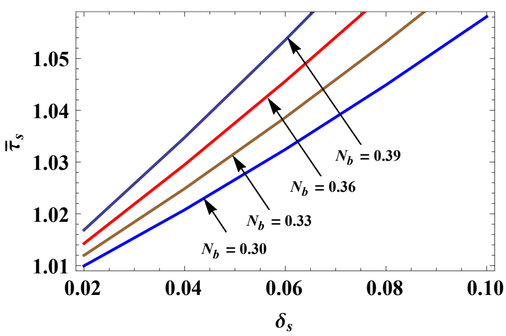

Figure 16. Effect of δ_s on $\bar{\tau}_s$ as N_b varies

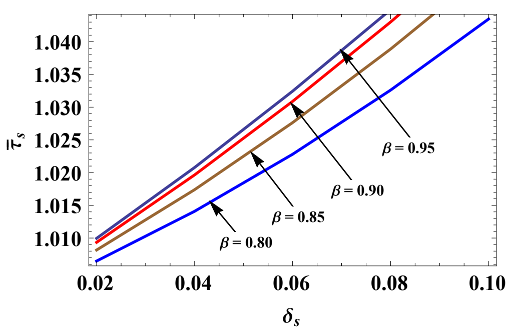

Figure 17. Effect of δ_s on $\bar{\tau}_s$ as β varies

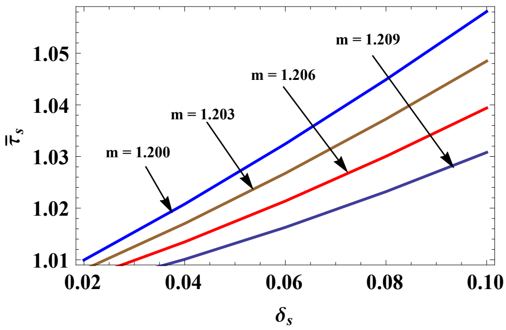

Figure 18. Effect of δ_s on $\bar{\tau}_s$ as m varies

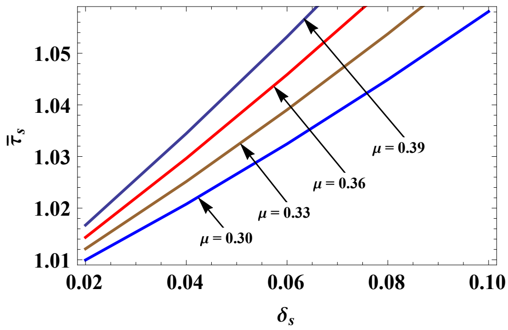

Figure 19. Effect of δ_s on $\bar{\tau}_s$ as μ varies

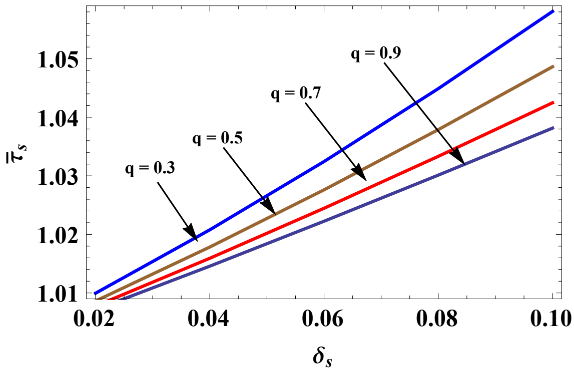

Figure 20. Effect of δ_s on $\bar{\tau}_s$ as q varies

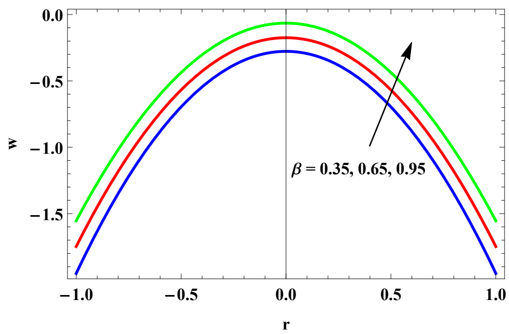

Figure 21. Variation of w with β

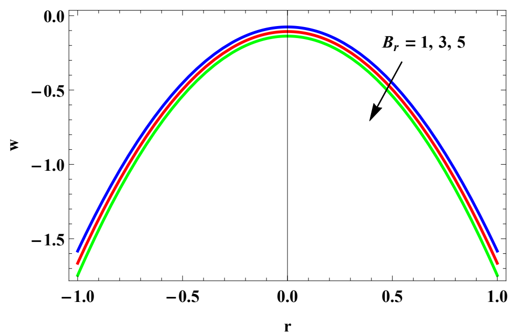

Figure 22. Variation of w with B_r

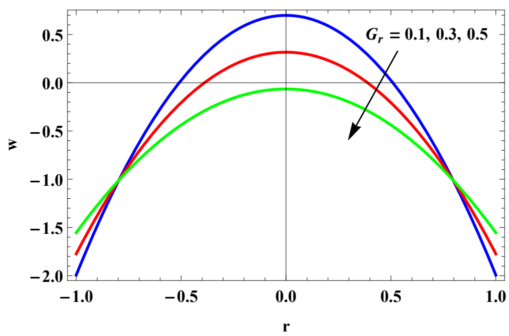

Figure 23. Variation of w with G_r

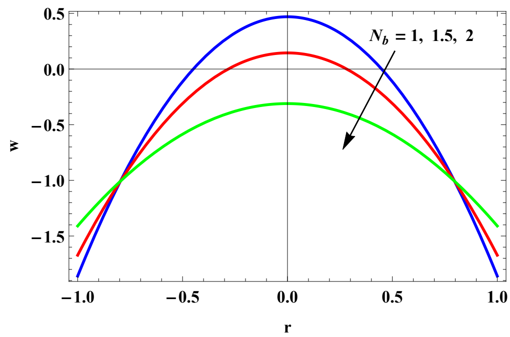

Figure 24. Variation of w with N_b

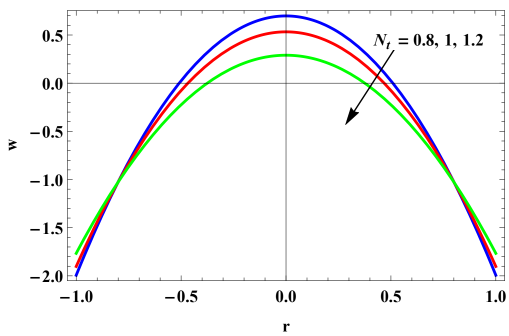

Figure 25. Variation of w with N_t

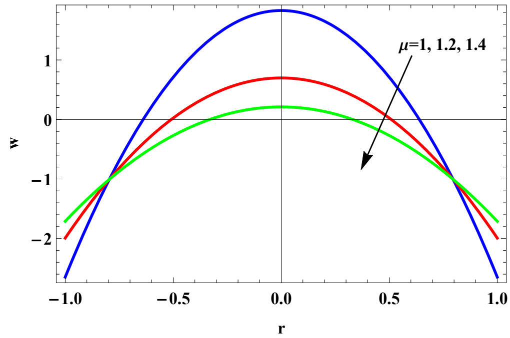

Figure 26. Variation of w with μ

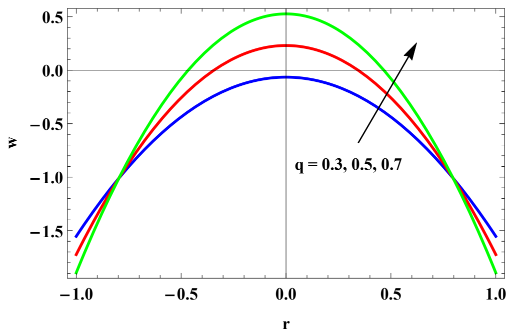

Figure 27. Variation of w with q

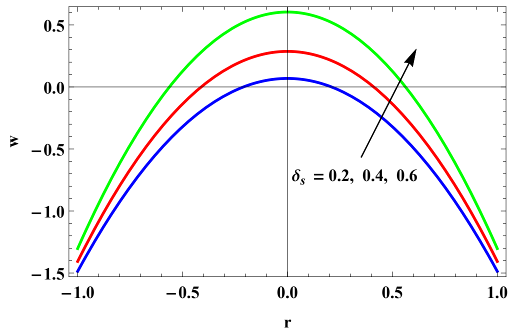

Figure 28. Variation of w with δ_s

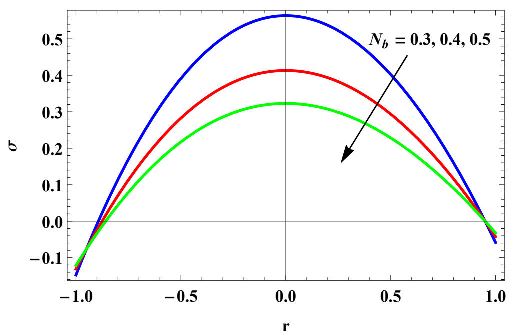

Figure 29. Effect of N_b on σ

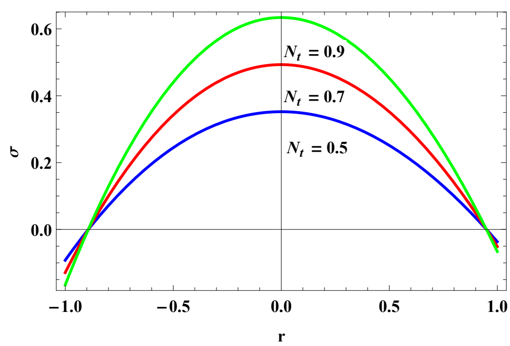

Figure 30. Effect of N_t on σ

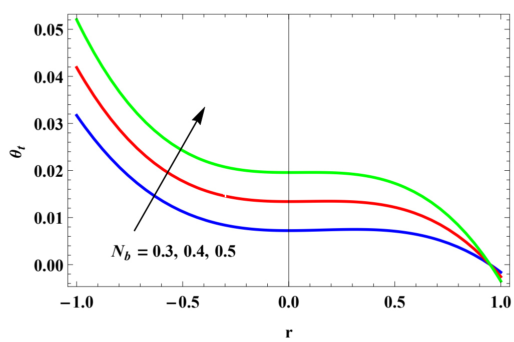

Figure 31. Effect of N_b on θ_t

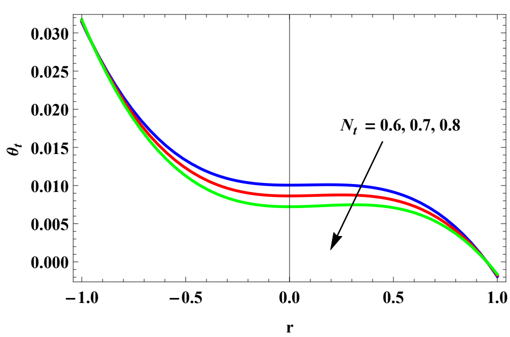

Figure 32. Effect of N_t on θ_t

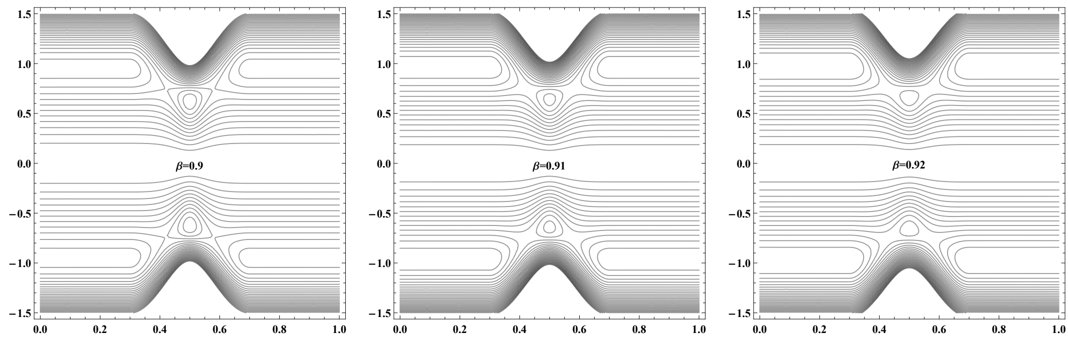

Figure 33. Streamlines for $\beta = 0.9, 0.91$ and 0.92

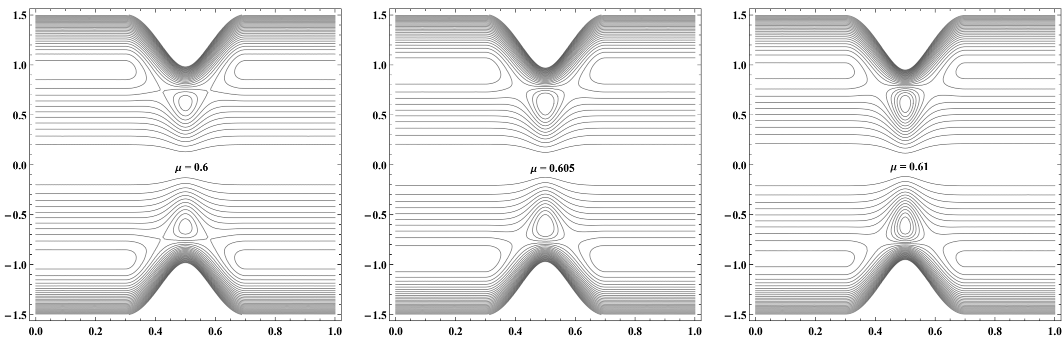

Figure 34. Streamlines for $\mu = 0.6, 0.605$ and 0.61

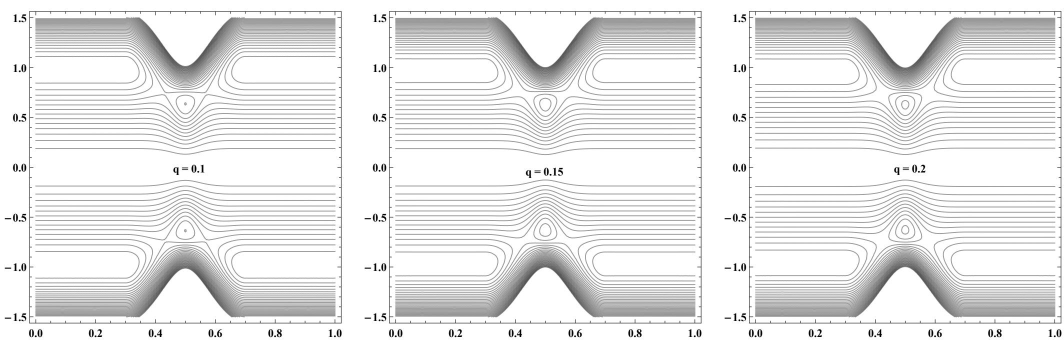

Figure 35. Streamlines for $q = 0.1, 0.15$ and 0.2

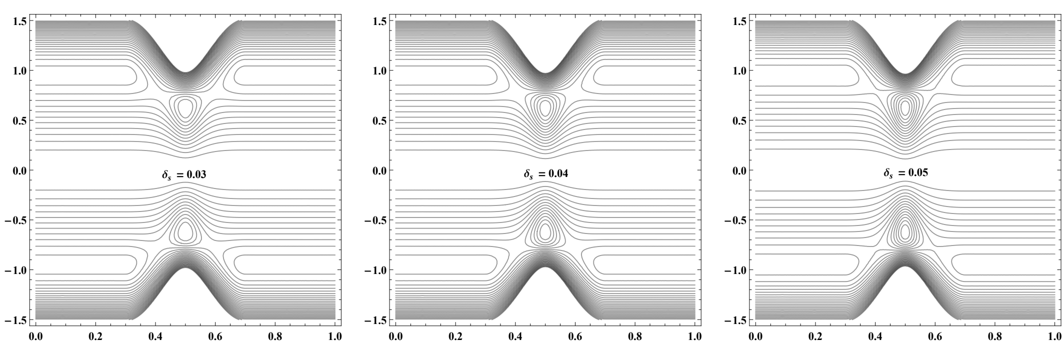

Figure 36. Streamlines for $\delta_s = 0.03, 0.04$ and 0.05

5 Conclusions

A two-layered mathematical analysis for a micropolar fluid having nanoparticles flow in the core region is considered to study the effects of fluid flow characteristics assuming mild stenoses. The characteristics like resistance to the flow $(\bar{\lambda})$, shear stress at surface of tube $(\bar{\tau}_s)$, concentration (σ) and temperature profile (θ_t) are the important characteristics in analyzing the fluid flow across a stenosed artery.

The conclusions based on the present study are:

(i) The flow impedance enhances by shape and size of the stricture for Stenoses heights, $B_r,\ m,\ \beta$ and, but found decreases with $G_r,\ N_t,\ q,\ \mu$. Also, it is seen that, the resistance to the flow decreases with N_b, which represents that collision between the molecules.

(ii) The wall shear stress which enhances with the rise in the values of $G_r,\ N_t,\ N_b,\ \beta,\ \mu$, but decreases with heights of the stenosis, $B_r,\ m,\ q$.

(iii) The profiles of velocity in the core region increase along the radial direction with the rise of q and β, but decreases with the increase of $B_r,\ G_r,\ N_b, N_t$ and μ.

(iv) The concentration profile due to presence of micropolar fluid having nanoparticles in core region is decreases with N_b, but increases with N_t.

(v) Temperature profile increases by enhancing N_t, whereas it decreases by enhancing N_b.

(vi) The streamlines for distinct values of $\beta,\ \mu, q$ and δ_s. It is seen that, as the value of β increases, the area of the boluses expands, but the quantity of boluses is decreased.

(vii) It is observed that, the area of the boluses expands and the quantity of boluses are increased with the increase of viscosity (μ) of the fluid and flux.

(viii) It is also noted that, with the increase of stenoses height of the core region, the area of the boluses is gradually decreased, but number of bolus is increased.

References

[1] Shukla, JB and Parihar, RS and Rao, BRP, Effects of stenosis on non-Newtonian flow of the blood in an artery, *Bulletin of Mathematical Biology* **42(3)**, 283–294 (1980).

[2] Sankar, DS and Hemalatha, K, Pulsatile flow of Herschel–Bulkley fluid through stenosed arteries—a mathematical model, *International Journal of Non-Linear Mechanics* **41(8)**, 979–990 (2006).

[3] Segers, Patrick and Verdonck, Pascal, Role of tapering in aortic wave reflection: hydraulic and mathematical model study, *Journal of biomechanics* **33(3)**, 299–306 (2000).

[4] Berger, SA and Jou, Liang-Der, Flows in stenotic vessels, *Bulletin of Mathematical Biology* **32(1)**, 347–382 (2000).

[5] Moayeri, MS and Zendehbudi, GR, Effects of elastic property of the wall on flow characteristics through arterial stenoses, *Journal of Biomechanics* **36(4)**, 525–535 (2003).

[6] Marshall, Ian and Zhao, Shunzhi and Papathanasopoulou, Panorea and Hoskins, Peter and Xu, X Yun, MRI and CFD studies of pulsatile flow in healthy and stenosed carotid bifurcation models, *Journal of biomechanics* **37(5)**, 679–687 (2004).

[7] Prasad, K Maruthi and Yasa, Prabhaker Reddy, Effect of non-Newtonian fluid flow through a permeable non-uniform tube having multiple stenoses, *AIP Conference Proceedings* **2246**, 020051 (2020).

[8] Eringen, A Cemal, Theory of micropolar fluids, *Journal of Mathematics and Mechanics* , 1–18 (1996).

[9] Prasad, K Maruthi and Yasa, Prabhaker Reddy, Flow of non-Newtonian fluid through a permeable artery having non-uniform cross section with multiple stenosis, *Journal of Naval Architecture and Marine Engineering* **17(1)**, 31–38 (2020).

[10] Mekheimer, Kh S and El Kot, MA, The micropolar fluid model for blood flow through a tapered artery with a stenosis, *Acta Mechanica Sinica* **24(6)**, 637–644 (2008).

[11] Pralhad, RN and Schultz, DH, Two-layered blood flow in stenosed tubes for different diseases, *Biorheology* **25(5)**, 715–726 (1988).

[12] Devanathan, Rathna and Parvathamma, S, Flow of micropolar fluid through a tube with stenosis, *Medical and Biological Engineering and Computing* **21(4)**, 438–445 (1983).

[13] Prasad, K Maruthi and Yasa, Prabhaker Reddy, S, Micropolar Fluid Flow in Tapering Stenosed Arteries having Permeable Walls, *Malaysian Journal of Mathematical Sciences* **15(1)**, 157–171 (2021).

[14] Srivastava, VP, Two-phase model of blood flow through stenosed tubes in the presence of a peripheral layer: applications, *Journal of Biomechanics* **29(10)**, 1377–1382 (1996).

[15] Srivastava, VP and Saxena, M, Two-layered model of Casson fluid flow through stenotic blood vessels: applications to the cardiovascular system, *Journal of Biomechanics* **27(7)**, 921–928 (1994).

[16] Shukla, JB and Parihar, RS and Gupta, SP, Effects of peripheral layer viscosity on blood flow through the artery with mild stenosis, *Bulletin of Mathematical Biology* **42(6)**, 797–805 (1980).

[17] Srivastava, VP, Flow of a couple stress fluid representing blood through stenotic vessels with a peripheral layer, *Indian Journal of Pure and Applied Mathematics* **34(12)**, 1727–1740 (2003).

Author information

K. Maruthi Prasad, Department of Mathematics, School of Science, GITAM (Deemed to be University), Hyderabad, Telangana State, India.
E-mail: maruthiprasadkaranamu@gmail.com

Bheema Sreekala, Research Scholar, Department of Mathematics, School of Science, GITAM (Deemed to be University), and Department of BS&H, BVRIT Hyderabad College of Engineering for Women, Hyderabad, Telangana State, India.
E-mail: bheemasreekala@gmail.com

Prabhaker Reddy Yasa, Department of BS&H, B V Raju Institute of Technology, Narsapur, Telangana State, India.
E-mail: prabhakerreddy.yasa@gmail.com

Received: September 12, 2021.
Accepted: March 7, 2022.